

Exploring the Usefulness of Varactor loaded Nonlinear Transmission Lines

Maseeh College of Electrical and Computer Engineering

Portland State University

Eric Aki

Juan Rivera-Mena

Jianyu Hao

Abstract—In this paper we will discuss the use of nonlinear elements within a transmission line to study their effects on the speed and shape of an input pulse, and how the next group which takes over our work may use this information to design similar circuits with improved bandwidth and/or performance.

I. INTRODUCTION

The goal of this project was to explore how non-linear transmission lines behave when loaded with varactors and how they can be used. Using design methodologies taken from previous studies and IEEE research, we have constructed a varactor loaded transmission line and attempted to observe and replicate the pulse sharpening effect shown in the literature.

First, we discuss the necessity of non-linear components in such a Nonlinear Transmission line or *NLTL* for short. We then discuss ways in which the devices we use in simulation are modeled and the obstacles we faced in constructing these models. We simulate these nonlinear lines using MICROCAP and discuss possible reasons for the discrepancies we have seen between research and simulations.

To verify the characteristic capacitance-voltage or CV curves of our chosen components, we construct a simple test fixture and measure capacitance vs. voltage using a DC power supply to reverse bias the varactor diodes and a handheld LCR meter.

II. THEORY

A. Why use Nonlinear Devices?

Non-linear devices in transmission lines have been widely used for pulse sharpening in particular. Similar sharpening can be observed by use of non-linear inductors and theoretically by strategic placement of dielectric material in the line [1]. The non-linearity helps us because it allows for voltage dependence impedance on the line. When an input pulse is sent through such a line, the voltage dependence causes a change in line impedance and a change in the behavior of the lumped element stubs which are also essentially low pass filters.

Much like a wave travelling in the ocean towards the shore, certain sections of the wave travel at different speeds despite the travel of the wave as a whole. This can be seen first hand

by a surfer utilizing their position on the wave to have the right speed and stability.

In electronics this same concept is present in optical fibers or waveguides. As we reflect a signal beam into a guide, the phase velocity can actually exceed the speed of light, however the speed of the the information characterized by the group velocity is what we care about.

B. Types of NLTL waves

While treating the physics of non-linear waves is beyond the scope of this paper, the use of NLTL's in transmission lines is founded upon the existence of waves that do not behave like the pure sine waves we usually consider in electronics. These both types of waves can be present and used in technology to lessen the time it takes for an input waveform to reach its final value as well as lessen the time to return to its “off” voltage state. In other words, these can be used to sharpen both rising and falling edges of a square wave input [2].

Informally, *Solitons* are much like the type of wave we see travelling in the open ocean without breaking and are characterized by their ability to interact with other waves without losing energy. This means that after passing another wave it largely maintains its shape and is only shifted in phase (experiences time delay).

Shockwaves are more easily visualized by a wave approaching the shore and breaking. This is the type of wave we utilize when considering non-uniform NLTL's. As the wave moves closer to the beach and the shoreline rises dramatically, the wave can no longer move in the same way due to the shore interrupting the circulating water and the momentum carried by it. With this sudden discharge of energy, we see the wave “break” and momentarily create a large vertical column of water.

C. Non-linearity vs Wave Dispersion

Another main concept of operation of these types of circuits, is the need for non-linearity to outweigh possible wave dispersion. Dispersion is a concept commonly discussed relative to optical fiber cable as a limiting factor of transmission speed. The idea is that travelling through any medium will cause a small amount of pulse spreading. This means that, if dispersion is strong enough, the pulse can spread or even break apart into several smaller pulses. To overcome this, we need enough

nonlinearity in the line primarily in terms of voltage/amplitude dependence such that the wave remains narrow.

Figure 1 [3], shows how construction of NLTL's follows catch up theory and how pulse sharpening is achieved by these types of circuits.

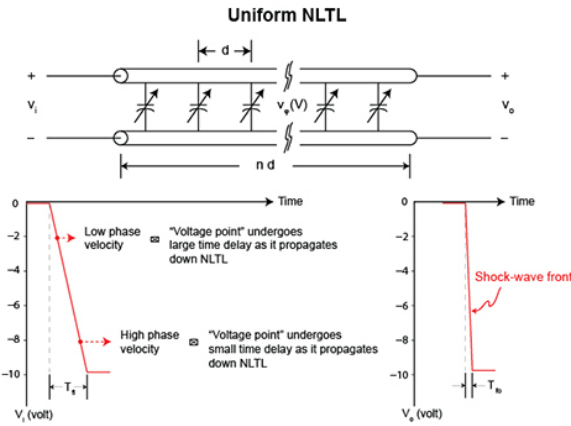


Figure 1. This graphic taken from an ANRITSU application note shows the basic principle of catch-up theory, and how it can be used to sharpen input pulses

D. Varactors vs. Nonlinear Capacitors

While nonlinear capacitors have been used in many studies [4] when implementing this design in high power systems, varactor diodes have the advantage of a larger capacitance range, and allow us to perform measurements using lower voltages. In addition, the overall design is simplified with the use of Varactors because only one bias is needed.

In any case, non linear capacitors are often modeled using equation (1) to describe the voltage dependence of the capacitance [5].

$$C(v) = \frac{C_0}{\sqrt{1 + v/V_0}} \quad (1)$$

where C_0 and V_0 are zero bias capacitance and reference voltage, respectively.

Equation (2) becomes useful as we start looking at larger pulses with large amplitude and should allow for scaling of our design.

$$C_{ls}(V_l, V_n) = \frac{1}{V_n - V_l} \int_{V_l}^{V_n} C(v) dv \quad (2)$$

This leads to an important constraint when designing passive NLTL's made up of series low-pass LC circuits. The fastest wave we can propagate down the NLTL can be approximately found by using equation (3) to find the cutoff frequency of the network as a function of the voltage across the varactors.

$$f_{bragg} \approx \frac{1}{2\pi\sqrt{LC(v)}} \quad (3)$$

This equation is used in section III-A indirectly to estimate the amount of pulse sharpening we can expect for a given step input

E. Methods of Modeling Varactors

In order to properly simulate and predict data using these simulations, we need first to determine how to model the non-ideal parasitics of the line and particularly the behavior of the chosen varactor diode loading the NLTL. There are several ways to accomplish this. The most standard and the method chosen by our group is SPICE modeling. The disadvantage of this route is that nonlinear behavior can be particularly hard to model with SPICE alone at higher frequencies and voltage levels (find source for this, think it's in SKYWORKS application note).

Another industry standard used to do this is by modeling via Verilog code. Specifically, Verilog-AMS or Verilog-A modules can more accurately capture the non-idealities in capacitors and varactors. This is a useful tool to explore as it can be integrated with many commercial simulation programs such as ADS.

F. Modeling Board Characteristics

When constructing a test fixture for measurements of NLTL's of higher frequency, we must also take into account the properties of the board we are working with. For our low frequency model and with limited access to robust VNA's this procedure was not necessary but we recommend using the two-line pencil method to approximate the board permittivity and loss tangent as utilized to do the same for flex PCB's due to its simplicity and limited need for equipment [6].

For our board, we used a simpler method which may prove useful as a quick and dirty alternative to the one described above. To find the permittivity of the board we used a simple LCR Meter (DE-5000) and the following formula of a parallel plate capacitor as shown in equation (4).

$$C = \frac{\epsilon A}{d} \quad (4)$$

Where we treat the width of the dielectric as plate spacing d , the board area as area, A , and measured capacitance as C . Solving for permittivity ϵ , we found a relative permittivity of $\epsilon_r \approx 3.54$. For this measurement a figure normally given for FR4 is roughly 4.0 to 4.4. A few possible things could cause this error.

The device used to measure the FR4 board generates a test frequency of 100kHz at maximum. Relative permittivity is usually given for FR4 at a much higher frequencies in the MHz range. Another is the precision achievable when measuring the dielectric thickness. A caliper would be much better suited for this task. Alternative methods do exist and are quite simple but do necessitate access to a VNA [7].

1) *SPICE Models:* SPICE models are typically easier to find and use in most circuit simulation software and what we used for our low frequency prototype as it seemed to be sufficient for our purposes. We chose to use software from the company SpectrumSoft. We chose this tool due to its vast array of built-in SPICE models and capabilities. For example, it ships with SPICE models for the BBY40 and SMV1249 varactor diodes. Previously a software found in industry for a high price, SpectrumSoft is now no longer in business and

has released this program free. It can be downloaded from SpectrumSoft's home page.

Additionally, the SPICE model for the hyper-abrupt varactor SMV1249 is found in application notes from their manufacturer, SKYWORKS Inc.

2) *Verilog-A Modules:* We were unable to utilize this modeling method. In section VII, we go over some potentially useful references to help you create models for higher frequency/bandwidth designs. Most verilog modules we have come across utilize equation 1 in order to model non-linear capacitors and varactors.

III. SIMULATIONS

In this section we will discuss the basics behind catch-up theory [1] and how we confirmed this with simulation. ΔT represents the time delay at the N^{th} node and is found by the difference period the line cutoff frequency at zero-bias varactor capacitance and the period of the line cutoff where varactor capacitance if defined by the step input maximum. This result is multiplied for every ladder section the pulse passes. Catch-up theory suggests that this delay is accounted for the variation in phase velocity as the rising pulse effects the varactor capacitance.

A. Simulating Rise Time

In our simulations we use an input step of 5 volts which takes $1\mu s$ to reach it's final value. Using equation (5), we calculate a pulse sharpening of $8.44ns$ at our 10^{th} node and $84.37ns$ at our 100^{th} node. To make these calculations, we used the CV plots obtained by measuring the BBY40 with the test fixture discussed in section V-A.

$$\Delta T = N(\sqrt{LC_o} - \sqrt{LC_s}) \quad (5)$$

For a lossless line, the sharpest pulse we can achieve can be estimated by first using equation 6 [1]. We notice that this utilizes the equation of our estimated bragg frequency as seen in (3) and describes the difference in cutoff frequencies at maximum and minimum bias voltage multiplied by the number of sections, N .

This gives us the ideal cutoff frequency of the line which in Hz is about $f_c \approx 290MHz$. The period of a wave moving at this rate is $T \approx 3.4ns$. While we have not been able to achieve a rise time of this magnitude, we need to remind ourselves of the inherent parasitics we are dealing with. Using a basic model with values from our inductor and varactor diode datasheet. We have a per section series resistance of roughly $R_s = 122m\Omega$ at DC, and a parallel resistance given by the resistance inherent in the varactor packaging as well as of the trace itself. This value was taken from the SPICE model used and was $R_p = 1m\Omega$

$$\omega_c = \frac{2}{\sqrt{LC_s}} \quad (6)$$

In figure 2 we can see that when simulating our ideal line, equation 5 is proven to be a very rough estimate to what we see. while at the 10^{th} section, we see a very similar value of

about 6ns compared to the $8.4ns$ calculated earlier, at the 100^{th} section we see about half of the expected pulse sharpening with our simulated value of $45ns$ compared to $84ns$ calculated.

At this time, we are unsure as to what has caused the discrepancy between calculation and simulation but we suspect it may have to do with our inability to properly model the nonlinear nature of the varactor diodes.

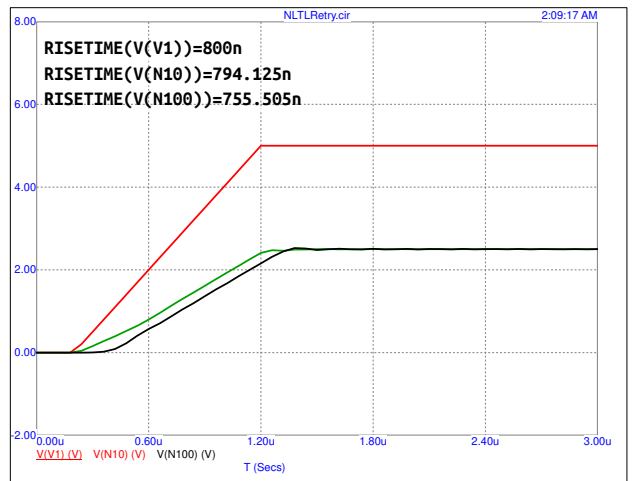


Figure 2. Rise time at source, node 10 and node 100 simulated with no resistive loss

In figure 3, we add the series DC resistance of the inductor ($R_s \approx 122m\Omega$) and the $1m\Omega$ resistance of the BBY40. From this, we see that not much has changed in this model and in fact we see an increased sharpening effect if anything. We do notice however, that the amplitude of the wave is much more attenuated at our 100^{th} node. This would lead us to expect a decrease in the pulse sharpening in the circuit instead of a relatively constant value due to the lessened effect on varactor capacitance as the pulse climbs.

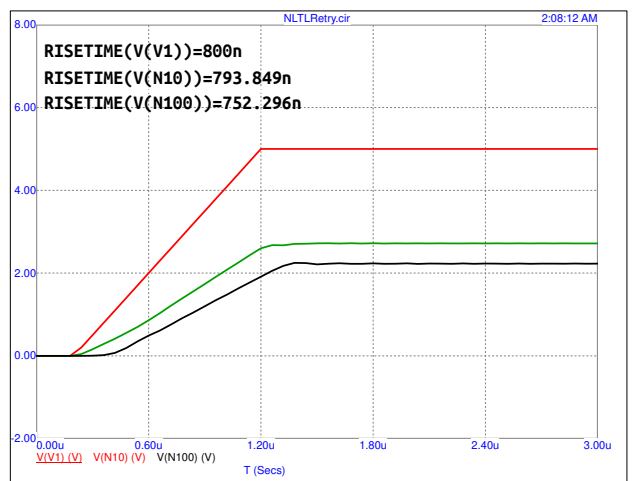


Figure 3. Rise time at source, node 10 and node 100 simulated with resistive loss of 0.122Ω per ladder section

Figure 4 explores the effect of different biasing on our line as well as how long a line we can practically use for sharpening purposes. As our DC resistance grows with our

line length, we expect our amplitude to keep dropping. As the amplitude of the traveling wave is reduced, we effectively trace out less of our varactor CV curves. Due to this, the CV relationship will begin to look more and more linear as we add ladder sections to our design. We have used a parametric plot to show the limits of this pulse sharpening as we increase the line length and plotted rise-time vs. DC bias for each 10th node of the ladder. The input pulse used in this case was 400ns.

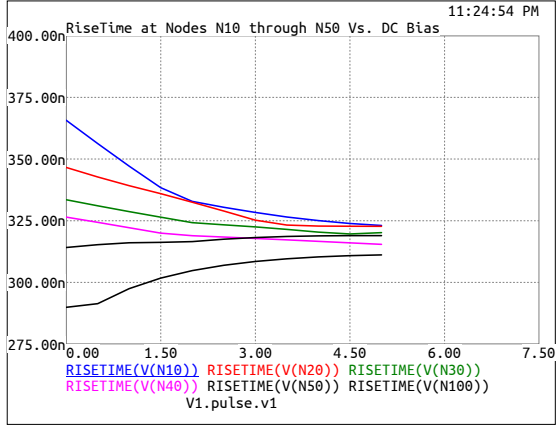


Figure 4. Risetime Vs. Line Length vs. DC Bias Voltage

IV. BOARD DESIGN

In order to test all these simulated values we designed a discrete version of our transmission line using Altium Designer. We emphasized traces being as short as possible and used Altium's built-in impedance profile tool to match our path between each pair of SMA connectors to 50Ω. The circuit we constructed is shown assembled in figure 5.

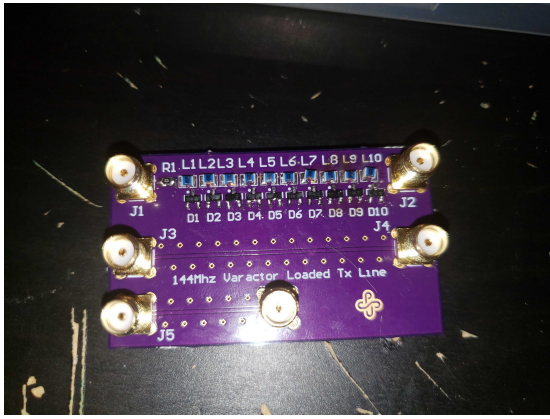


Figure 5. Assembled Tx Line Board made for 144Mhz

V. MEASUREMENT RESULTS

A. Varactor CV Curves

To measure and find the capacitance vs Voltage of our chosen varactors we created a small ugly style circuit based on a design by W2AEW. Two 100k resistors are added to limit

current flowing to the power supply. A ceramic capacitor of value much greater than our varactor is placed to protect the meter from excessive voltage. Since this larger capacitance is in effectively in parallel with our varactor, our meter measurement is approximately only the capacitance of the varactor diode itself.

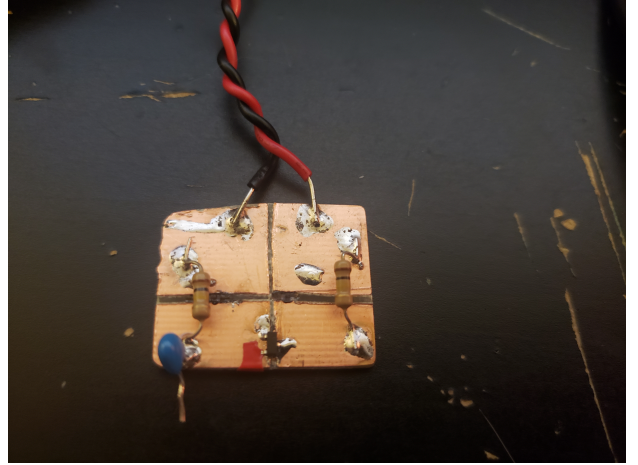


Figure 6. Test Fixture used for plotting CV Curve of BBY40

Through use of this fixture, we were able to generate the curves shown in figures 7 and 8. These were in close agreement to curves found on datasheets for the BBY40 and SMV1249 respectively.

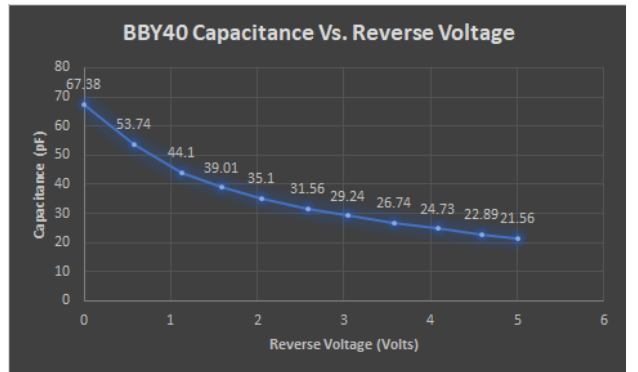


Figure 7. Measured CV Characteristics of BBY40

B. AC Response

C. Rise Time

We had great difficulty in measuring rise time of our circuit and the main problems we faced were not understanding the theory well enough have do proper testing. While our components were chosen on the basis of working at 144Mhz, we failed to see that driving our circuit below this bandwidth and performing similar simulations may be adequate to prove rise time performance increase. Another complication was keeping in mind the biasing conditions of the varactors. We did not design for a port in which to introduce a dc bias to our circuit and relied on equipment being able to accomplish this. Care must be taken when using analog generators to

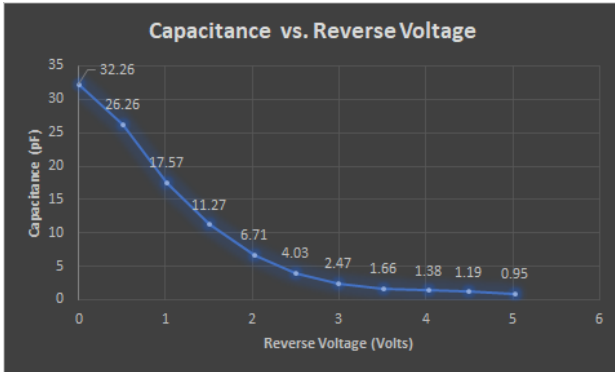


Figure 8. Measured CV Characteristics of SMV1249

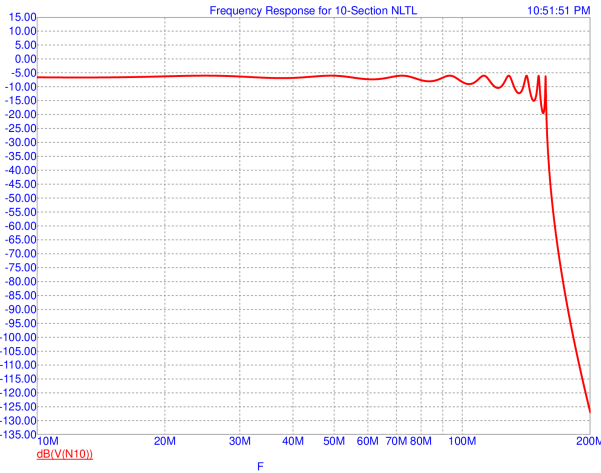


Figure 9. Simulated AC Response for Board 1

supply the DC bias to the circuit. Our particular model begins sweeping with a negative bias before reaching a positive one. This effectively puts the varactors into forward bias and allows them to hold a charge.

D. S-parameters

In figure 19 shows the schematic used to measure and compare our measured s-parameters taken through a NanoVNA to

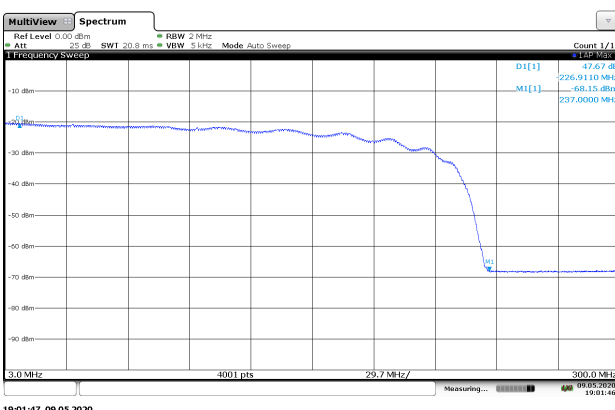
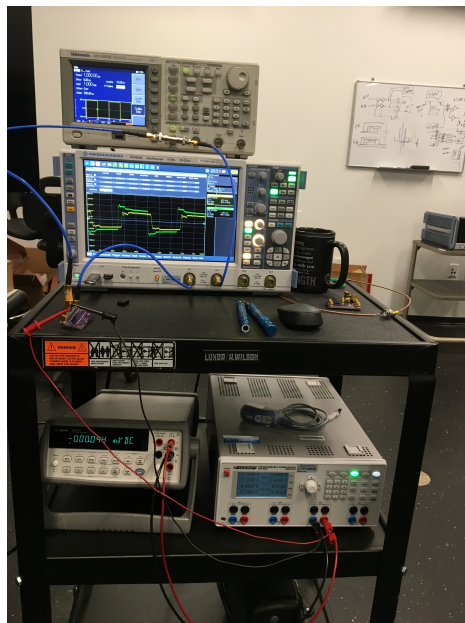
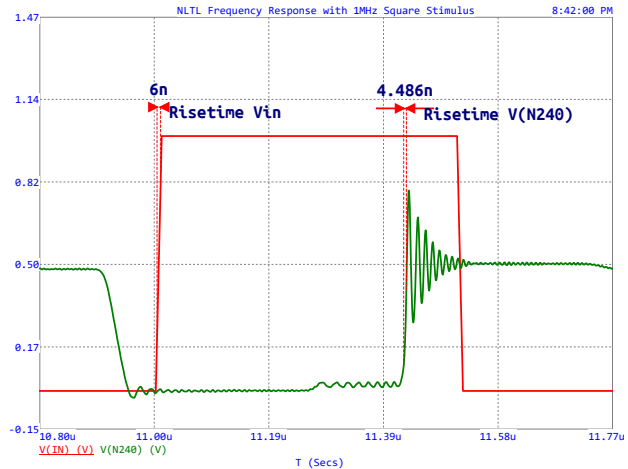
Figure 10. Measured Frequency Response for Board 1 ($L = 56\text{nH}$)

Figure 11. Test Setup for Measuring Risetime With Bias

Figure 12. Simulated Risetimes for Input pulse, 10th node, and the 240th node

our simulated circuit with parasitics included. The NanoVNA data is imported through use of the n-port components and define statements are utilized to calculate other parameters such as generated power in dbm, VSWR, etc...

To produce figure 20, we parameterized the values of our parasitic elements in circuit and within the BBY40 model itself. We changed these values to match our measured data more closely to see the accuracy of our model. While we were able to achieve relatively agreeing data we still see a large discrepancy in our S11 data. At 10MHz, we see a our measured data is roughly -10dbm lower than our expected simulation. This could be due to incorrect modeling of our load impedances and requires further study. Some have mentioned that when using NLTL's, there is bound to always be some impedance mismatch due to the changing impedance caused by varactor capacitance [1]. This may be the case here, but the issue is worth further simulation.

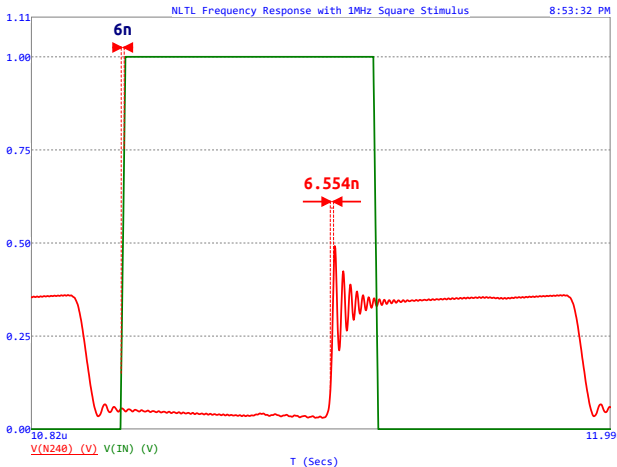


Figure 13. Accounting for Series Resistance shows that there is a certain point where no more sharpening takes place



Figure 14. Risetime Measurement from Board 1 ($L=56\text{nH}$)

In figure 21, we see that our measured and simulated are almost identical except for a sharp rise in VSWR near the resonant frequency of our LC network (144Mhz). After this point, we expect our VSWR to start rising dramatically. What we see is a much more subtle increase from about 1.5 to 5. Still a much larger ratio than was present within our operating bandwidth, but certainly not the expected value of ≈ 100 .

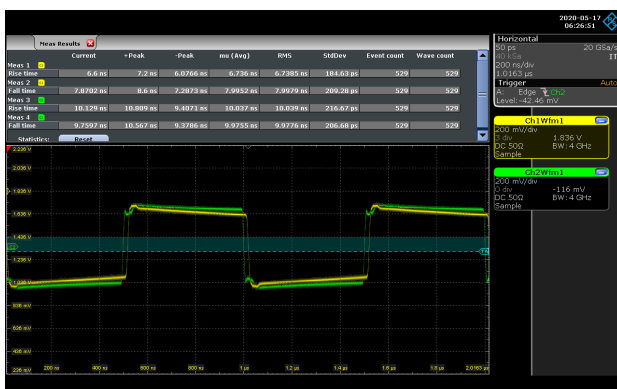


Figure 15. Measured Risetime with 1V DC Bias



Figure 16. Measured Risetime with 2V DC Bias

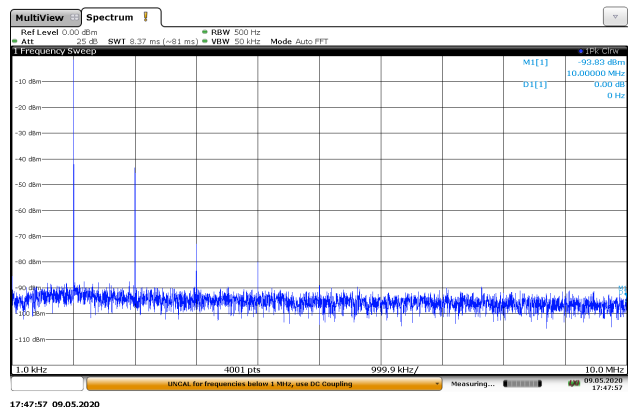


Figure 17.

VI. MODEL ACCURACY/ PREDICTIONS

Under Construction: Using this section for generating bibliography for the time being. We will work on predictions and further flesh things out during the next revision. [8] [9], [10], [11], [12], [13], [4], [5], [6], [14]

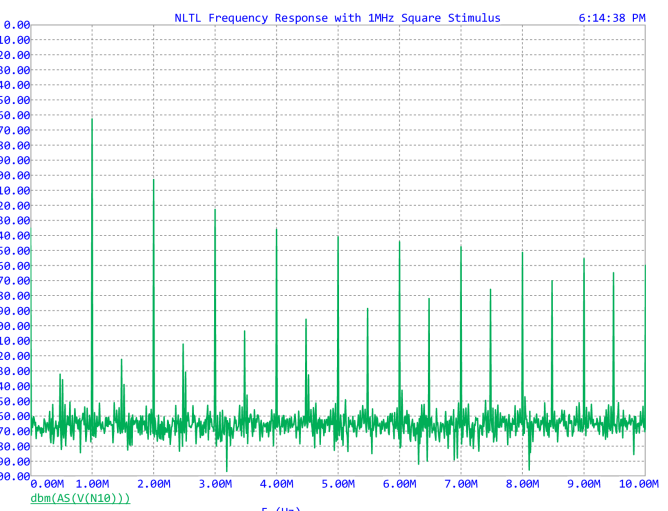


Figure 18. Expected Power Spectrum when DUT fed with 1Mhz 1Vpp Sine Wave

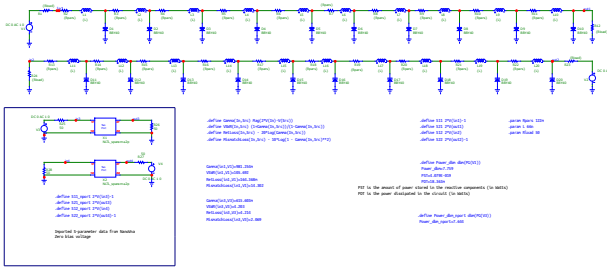


Figure 19. Schematic used to generate S-parameter plots. The top line measures S11 and S12, and bottom line measures S21 and S22.

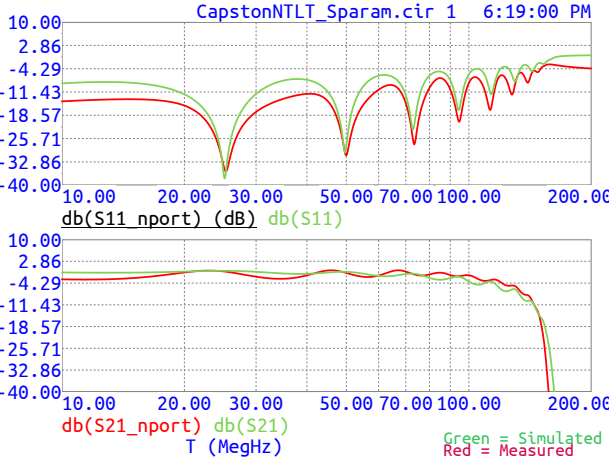


Figure 20. Simulated vs. Measured S_{11} and S_{21} . Corrections to make on next draft include more sensible scaling of axes

A. Estimating Circuit-Q

To estimate our circuit Q, we employ a technique called ring-down method [15]. Driving the circuit with a square wave much slower than the expected resonance frequency of the LC network, we simply count the amount of cycles it takes for the signal envelope to decay to roughly 50% of the maximum amplitude. Observing figure /reffig:EstimatingQ, we see that the ringing dies down in about 1 cycle. To get our Q estimate,

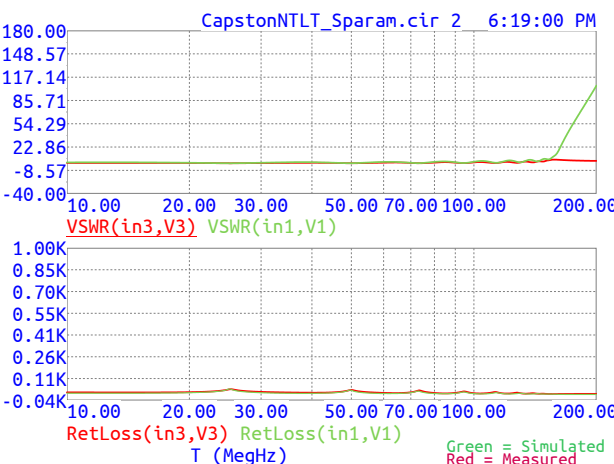


Figure 21. Simulated vs. Measured Return Loss and VSWR



Figure 22. Transient Waveform for Estimating Q

we simply multiply this value by approximate 4.53. This yields an approximate Q of 4.53 for our transmission line. This seems a little lower than expected however, we can see that the ringing is not as clean as we expected. It is unsurprising that our non-linear circuit results in a fluctuating impedance on the line causing reflections and is prone to generating harmonic content.

By feeding in a 1Vpp Sine wave and measuring the frequency response of our circuit, we see that many harmonics should be present in our line. Since we are using this simulation to stand in place of a physical measurement, this interference makes sense.

To repeat this process for our physical circuit is a good next step to confirm the observed value of $Q \approx 5$.

VII. NEXT STEPS

A. Verilog-A Module

While we were able to draft a preliminary Verilog-A module for this project, we were unable to fully debug, implement, or optimize this code. Introductory literature exists explaining how these models are constructed and used [16]. There also exists literature specifically gear toward creating RF models using Verilog-A [17].

B. Using varying physical circuit geometry

figure 23 shows a possible implementation of pulse sharpening by taking advantage of the circuit's physical geometry to produce further non-linearities and mismatches in the circuit. This type of geometry should be used with much higher frequencies than the designs we created for this report as it relies on the the lines themselves to act as inductive components. This exploration may have several advantages including easier reproduction and less resistive losses on the line due to lack of discrete inductors.

As an intermediate step, it may be beneficial to conduct further simulation with varied inductance and parasitics to emulate the behavior of this topology. "non-uniform" topologies have other applications and some examples can be found in spectroscopy [18] with use as antenna tuners [19] or even in bandpass filter designs [20].

VIII. CONCLUSION

REFERENCES

- [1] C. R. Wilson, M. M. Turner, and P. W. Smith, "Pulse sharpening in a uniform lc ladder network containing nonlinear ferroelectric capacitors," *IEEE transactions on electron devices*, vol. 38, no. 4, pp. 767–771, 1991.

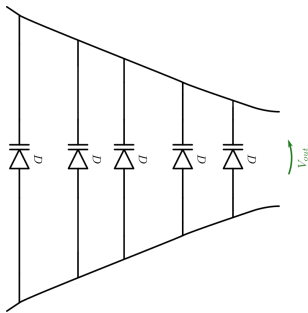


Figure 23. Potential circuit geometry to be simulated and built going forward

- [2] E. Afshari and A. Hajimiri, “Nonlinear transmission lines for pulse shaping in silicon,” *IEEE Journal of Solid-State Circuits*, vol. 40, no. 3, pp. 744–752, 2005.
- [3] “Shockline ntl,” 2020. [Online]. Available: <https://www.anritsu.com/en-us/test-measurement/technologies/shockline-ntl>
- [4] S. Ibuka, K. Abe, T. Miyazawa, A. Ishii, and S. Ishii, “Fast high-voltage pulse generator with nonlinear transmission line for high repetition rate operation,” *IEEE Transactions on Plasma Science*, vol. 25, no. 2, pp. 266–271, 1997.
- [5] M. S. Nikoo, S. M.-A. Hashemi, and F. Farzaneh, “Theory of rf pulse generation through nonlinear transmission lines,” *IEEE Transactions on Microwave Theory and Techniques*, vol. 66, no. 7, pp. 3234–3244, 2018.
- [6] F. Declercq, H. Rogier, and C. Hertleer, “Permittivity and loss tangent characterization for garment antennas based on a new matrix-pencil two-line method,” *IEEE Transactions on Antennas and Propagation*, vol. 56, no. 8, pp. 2548–2554, 2008.
- [7] A. Namba, O. Wada, Y. Toyota, Y. Fukumoto, Zhi Liang Wang, R. Koga, T. Miyashita, and T. Watanabe, “A simple method for measuring the relative permittivity of printed circuit board materials,” *IEEE Transactions on Electromagnetic Compatibility*, vol. 43, no. 4, pp. 515–519, 2001.
- [8] M. Ould-Elhassen, M. Mabrouk, A. Ghazel, and P. Benech, “Circuit simulation of varactor loaded line phase shifter,” in *Progress in Electromagnetics Research Symposium Proceedings.-2011*, 2011.
- [9] A. S. Nagra and R. A. York, “Distributed analog phase shifters with low insertion loss,” *IEEE Transactions on Microwave Theory and Techniques*, vol. 47, no. 9, pp. 1705–1711, 1999.
- [10] F. Ellinger, H. Jackel, and W. Bachtold, “Varactor-loaded transmission-line phase shifter at c-band using lumped elements,” *IEEE Transactions on Microwave Theory and Techniques*, vol. 51, no. 4, pp. 1135–1140, 2003.
- [11] W. Lee, M. Adnan, O. Momeni, and E. Afshari, “A nonlinear lattice for high-amplitude picosecond pulse generation in cmos,” *IEEE transactions on microwave theory and techniques*, vol. 60, no. 2, pp. 370–380, 2012.
- [12] F. Ellinger, R. Vogt, and W. Bachtold, “Ultra compact, low loss, varactor tuned phase shifter mmic at c-band,” *IEEE Microwave and Wireless Components Letters*, vol. 11, no. 3, pp. 104–105, 2001.
- [13] D. Q. Xu and G. R. Branner, “An efficient technique for varactor diode characterization,” in *Proceedings of 40th Midwest Symposium on Circuits and Systems. Dedicated to the Memory of Professor Mac Van Valkenburg*, vol. 1, 1997, pp. 591–594 vol.1.
- [14] T. Tsuboi and F. M. Toyama, “Computer experiments on solitons in a nonlinear transmission line. i. formation of stable solitons,” *Phys. Rev. A*, vol. 44, pp. 2686–2690, Aug 1991. [Online]. Available: <https://link.aps.org/doi/10.1103/PhysRevA.44.2686>
- [15] I. Giangrandi. [Online]. Available: <https://www.giangrandi.org/electronics/ringdownq/ringdownq.shtml>
- [16] G. J. Coram, “How to (and how not to) write a compact model in verilog-a,” in *Proceedings of the 2004 IEEE International Behavioral Modeling and Simulation Conference, 2004. BMAS 2004.*, 2004, pp. 97–106.
- [17] B. Troyanovsky, P. O’Halloran, and M. Mierzwiński, “Analog rf model development with verilog-a,” in *2005 IEEE Radio Frequency integrated Circuits (RFIC) Symposium-Digest of Papers*. IEEE, 2005, pp. 287–290.
- [18] M. R. Palmer, B. R. Wenrich, P. Stahlfeld, and D. Rovnyak, “Performance tuning non-uniform sampling for sensitivity enhancement of signal-limited biological nmr,” *Journal of biomolecular NMR*, vol. 58, no. 4, pp. 303–314, 2014.
- [19] D. Cure, T. M. Weller, and F. A. Miranda, “Non-uniform bias enhancement of a varactor-tuned fss used with a low profile 2.4 ghz dipole antenna,” in *Proceedings of the 2012 IEEE International Symposium on Antennas and Propagation*. IEEE, 2012, pp. 1–2.
- [20] H. Guo, J. Ni, and J. Hong, “Varactor-tuned dual-mode bandpass filter with nonuniform q distribution,” *IEEE Microwave and Wireless Components Letters*, vol. 28, no. 11, pp. 1002–1004, 2018.